

UNIOSUN Journal of Engineering and Environmental Sciences. Vol. 2, No. 1. March. 2020

DOI: 10.36108/ujees/0202.20.0110

Low Pressure CO₂ Capture with Amide-Based Imprinted Polymers

Fayemiwo, K.A., Vladisavljević, G.T., Nabavi, S.A. and Manović, V.

Abstract: Bulk polymerization was used to fabricate molecularly imprinted polymer (MIP) adsorbents inherent with amine-functionality for post combustion CO₂ capture. Polymerization was performed at 333 K for 24 hours using methacrylamide and ethylene glycol dimethacrylate (EGDMA) as the functional monomer and cross linker respectively, oxalic acid as the template azobisisobutyronitrile (AIBN) as the initiator and 4:1 (v/v) mixture of acetonitrile and dimethylformamide (DMF) as the porogenic solvent. The monolithic polymers were crushed and ground, followed by screening to 75-215 µm and the template was then removed from the polymeric particles by extraction using methanol and hydrochloric acid (90/10 v/v). A fixed bed adsorption column was used to investigate the performance of the dynamic CO2 uptake capacities. The X-ray Photoelectron Spectroscopy (XPS) and Fourier Transform Infrared spectroscopy (FT-IR) spectra showed a huge number of -NH2 functionality distributed on the surface of the adsorbents, which thus enhanced the CO₂ adsorption uptake. The maximum CO₂ capture capacity was found in the MIP with the maximum template concentration (0.40 mmol/g, $S_{\rm BET}$ 258 m²/g at 0.15 bar partial pressure and temperature of 313 K). The MIPs were stable thermally up to 518 K and the isotherms displayed type II revealing a non-uniform distribution of the pore size.

Keywords: Climate change, CO2 uptake, amide-based, imprinted polymer, low-pressure

I. Introduction

The major greenhouse gas that poses a threat to the global environment is carbon dioxide (CO₂) emissions, which is largely because of human deeds and doings like the combustion of fossil fuels (coal, petroleum and natural gas) for transportation and energy. Increase in global warming has led to a dramatically change in climate, affecting the ecological system negatively, and this has been the greatest challenge the world is battling with. Researchers agreed globally that a reduction in CO₂ emissions into the air is of great necessity [1]–[4]. Therefore, there is need to develop technologies to capture CO₂ to reduce the effect of green house.

Fayemiwo, K. A. (Department of Chemical Engineering, Osun State University, Nigeria.)

Vladisavljević, G. T. Department of Chemical Engineering, Loughborough University, United Kingdom)

Nabavi, S. A. and Manović, V. (Centre for Climate and Environmental Protection, Cranfield University, United Kingdom)

Corresponding author: kehinde.fayemiwo@uniosun.edu.ng

In carbon capture and storage (CCS) technique, adsorption has been referred to as a promising CO₂ capture technique that is cost effective and energy efficient [5]. Several types of adsorbents have been employed in CO₂ capture; such as silica, activated carbon, and zeolites; however, they have their drawbacks based on selectivity, adsorption capacity and dehumidification requirements [5, 6, 7, 8]. These drawbacks have led to further studies which are being tailored towards the development of cheaper and more selective adsorbents for CO2 capture.

Recently, sufficiently great attention has been paid to the use of polymer-based adsorbents for CO₂ capture owing to their high CO₂ sorption capacity and acceptable CO₂ preferential selectivity over N₂; flexibility in structural modification, light weight, reusability and low energy for regeneration [8, 9, 10, 11]. More so, they have reasonably acceptable physicochemical, mechanical and thermal properties owing to their networks

covalent bonding nature [7]. For these reasons, they have been referred to as potential materials for practical CO₂ capture applications [12, 13].

Molecularly imprinted polymer (MIP) is a polymer that is fabricated through the molecular imprinting technique, by inducing molecular recognition properties in polymer [8, 14, 15]. MIP technique requires a functional monomer, template, initiator, cross-linker, porogenic and extraction solvent. The target molecule behaves like the template around which interacting and cross-linking monomers are arrayed and co-polymerized, to form a complex with the template, after which the binding sites would be exposed when the template is removed [16, 17, 18]. These binding sites are corresponding to the template in shape, size and functional group positions, thus, having ability to selectively rebinding the template [19, 20, 21]. Thus, the MIPs have the capability to identify and bind a particular target molecule.

Molecularly imprinted polymer (MIP) amide-decorated particles possessing CO₂ recognition nanocavities and has properties was reported to have been synthesized via suspension polymerization method [15]. The reported particles possessed S_{BET} of 457 m²/g and 0.92 cm³/g mesopore volume. The CO2 uptake ability was up to 0.56 mmol/g at $40 \, {}^{\circ}\text{C}$ (313 K), and CO_2 partial pressure of 0.15 bar. However, the MIPs were synthesized from a toxic and environmental unfriendly monomer, acrylamide.

In this work, amide-based imprinted polymers were produced from non-toxic monomer, methacrylamide crosslinked with EGDMA by bulk polymerisation for a low-pressure CO₂ capture. Bulk polymerisation was preferred as it eliminate the use of surfactant which can serve as a contaminant on the polymer by hindering the active surface area. The polymer particles produced were characterised and the CO₂ capture capacity were investigated. The

effect of porogenic solvents and cross-linker on the surface area and sorption capacity were also studied. Oxalic acid was used as a dummy template because it has a structural analogue similar to that of CO₂ molecules.

II. Experimental Section

A. Materials and Chemicals

Acetonitrile (AN), Hydrochloric Acid (HCl), Dimethylformamide (DMF) and Methanol were purchased from Fisher Scientific (UK). Ethylene glycol dimethacrylate (EGDMA), Methacrylamide (MAAM), Azobisisobutyronitrile (AIBN) and Oxalic acid (OA) were purchased from Sigma Aldrich (UK). All reagents were of analytical grade. Millipore 185 Milli-Q Plus apparatus was used to supply reverse osmosis (DI) water.

Gases used in this work were supplied by BOC (UK) and had purity higher than 99.99 %. The material characterisation techniques are as described in our former paper [22]. Micrometric ASAP 2020 Accelerated Surface Area and Porosimetry was used to investigate the nitrogen adsorption-desorption isotherms, specific surface area and the pore volume distribution. The thermal analysis was performed using a thermogravimetric analyser (TGA) (Q5000 IR, TA instruments, US) and the density of the particles was determined using a helium pycnometer (Micrometrics, US).

The Fourier transform infrared (FTIR) spectra were measured using a Thermo Scientific Nicolet iS50 ATR spectrometer and the X-ray photoelectron spectroscopy were performed on a K-alpha Thermo Scientific spectrometer using an Al Ka monochromatic X-ray source for radiation. The dynamic CO₂ adsorption of the adsorbents were investigated in a fixed-bed column made of stainless steel (details provided in the supplementary information, S1).

B. Synthetic Procedure

The fabrication of a series of imprinted polymers (SMP) adsorbents were carried out via bulk polymerisation using a 30 mL glass vial fitted with 20 mm rubber stopper and sealed. MAAM (functional monomer) and oxalic acid (template) were both dissolved in a mixture of AN:DMF (as porogenic solvent) and allowed to create monomer template selfassembly for 2 hours. After monomertemplate complex assembly, the cross linker, EGDMA and the initiator, AIBN were both added and dissolved. The mixture was degassed for 10 mins using ultrasonic device and then purged for an additional 10 mins with an inert N₂ atmosphere in order to eliminate oxygen. The glass vials were sealed and placed in closed hot water-bath at 333 K for 24 h to polymerise. The resulting polymer monoliths were ground and screened to 75 -The particles were continuously with HCl/methanol (1/9,vol/vol), to extract the template, until there were no significant traces of the template as tested using UV spectrometer; it was then filtered and dried overnight in the vacuum oven at temperature of 353 K. The removal of the template left behind a binding site that can easily rebind CO2 during adsorption. The non-imprinted polymer counterpart (SNIP) was also synthesized in the same manner without using the template. The conditions of the fabrication are as stated in Table 1.

III. Results and Discussion

A. Characterisation of the Polymer

Figure 1 shows the isotherms of the nitrogen adsorption-desorption at 77 K and the pore size distribution of the adsorbents. In accordance with IUPAC classification, all synthesized polymeric adsorbents displayed Type II isotherms [23]–[25]. This isotherm form is generally accustomed with microporous adsorbents [26]. At P/P₀ values of 0.1 or below, the monolayer was completed for all samples, and this was

succeeded by multilayer adsorption at higher values of P/P₀.

Table 1: The specific surface area, S_{BET} , the total pore volume (V_p) and pore size (d_p) of the adsorbents synthesised^a

Sample	MAA m	OA	EG DM A	S _{BE}	V_p	d_p
	g	G	g	m² /g	cm³/	nm
SMP-1	2.04	0.18	7.93	250	0.63	14.85
SMP-2	2.04	0.09	7.93	262	0.63	14.26
SMP-3	2.04	0.36	7.93	258	0.63	14.87
SNP	2.04	nil	7.93	217	0.72	16.76
SMP-4	1.02	0.18	7.93	399	0.76	10.18
SMP-5	3.06	0.18	7.93	162	0.47	13.49
SMP-6	2.04	0.18	6.00	173	0.47	15.06
SMP-7	2.04	0.18	9.90	272	1.55	23.00

^aFor all samples synthesised, the porogenic solvent was 16 ml of ACN and 4 ml of DMF, the polymerisation was carried out at 333 |K for 24 h.

The S_{BET} and pore volume (V_p) of the adsorbent was evaluated using the nitrogen adsorption isotherm, while average pore diameter (d_p) was determined using the equation, dp = $4V_p/S_{BET}$ [8]. The ranges of the pore size were found to be in between 2.5 nm and 40 nm, while all samples showed a clear-cut peak around 3.7 nm. The effect of an increase in template was not that noticeable in the S_{BET} , SMP-2 < SMP-1 <SMP-3 (0.09 < 0.18 < 0.36), as the S_{BET} ranged from 250 m²g⁻¹ to 262 m²g⁻¹. This was also revealed in the pore volume as it was ~ 0.63 cm³g⁻¹, and pore size likewise ranged 14.27 nm to 14.87 nm. However, clear differences exist between the imprinted (SMP-1) and the non-imprinted counterpart (SNP). The S_{BET}, pore volume and pore size for SMP-1 were 250 m²g⁻¹, 0.63 cm³g⁻¹ and 14.85 nm and for SNP it was 217 m²g⁻¹, 0.72 cm³g⁻¹ and 16.76 nm respectively. Thus, the template significantly increased the S_{BET}, but causes a reduction in both pore volume and pore size.

On the other hand, there was a notable effect of monomer concentration on the SBET

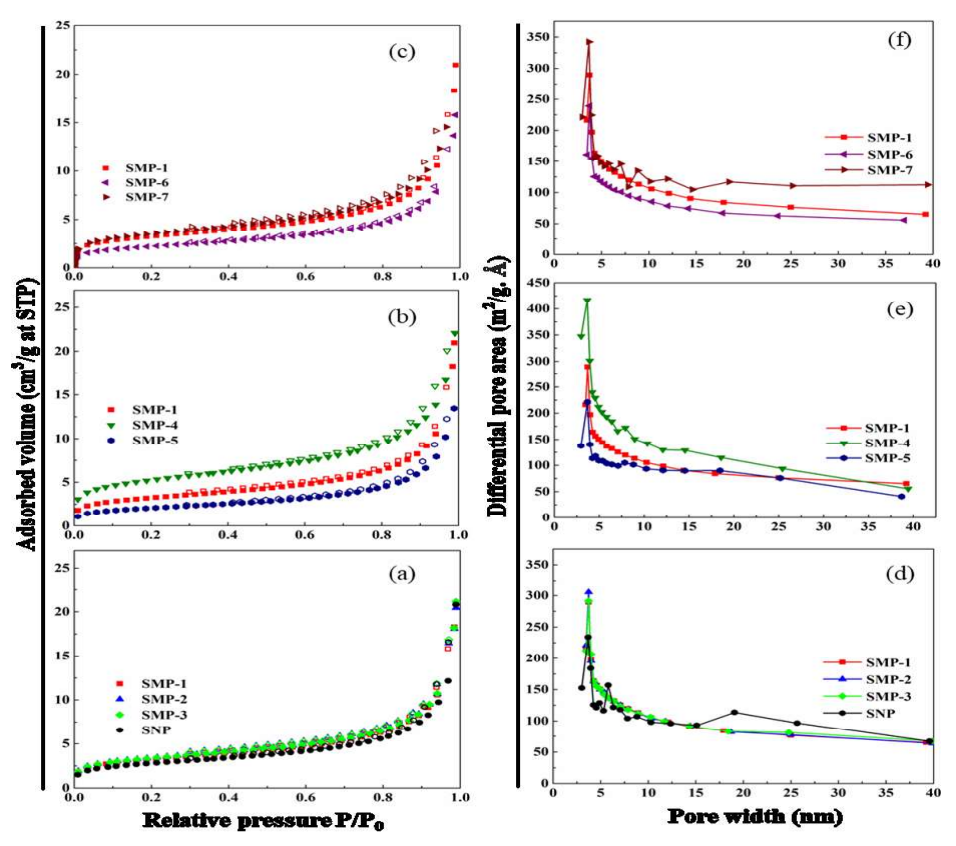


Figure 1: Nitrogen adsorption isotherms of the adsorbents particles at 77 K as a function of (a) template, (b) monomer and (c) crosslinker. The filled and empty symbols represent adsorption and desorption isotherms respectively. Mesopore size distribution curves of the samples based on (d)template, (e) monomer and (f) crosslinker.

(Table 1). An increase in monomer concentration from 2.04 g (SMP-1) to 3.06 g (SMP-5) led to a decrease in S_{BET}, 250 m²g⁻¹ to 162 m²g⁻¹ while a decrease in monomer concentration (SMP-4) lead to a notable increase of 399 m²g⁻¹. However, there was a significant effect of the crosslinker on the S_{BET} and pore size of the adsorbents synthesized. As the crosslinker increases, SMP-6 \leq SMP-1 \leq SMP-7, the S_{BET} also increases, $173 \text{ m}^2\text{g}^{-1} < 250 \text{ m}^2\text{g}^{-1} < 272 \text{ m}^2\text{g}^{-1}$ respectively, and the pore sizes likewise increase $0.47 \text{ cm}^3\text{g}^{-1} < 0.63 \text{ cm}^3\text{g}^{-1} < 1.55$ cm³g⁻¹ respectively. This effect can be as a result of decrease or increase in the degree of crosslinking of the polymers respectively [22].

Figures 2a, 3a and 4a represented the Fourier-transform infrared spectroscopy (FTIR) spectra of the samples with respect to variation in the concentration of template,

monomer and concentration respectively. For all adsorbents, the peaks at 3440 cm⁻¹ and 1635 cm⁻¹ can be attributed to N-H stretching and N-H bending vibrations respectively. This confirmed that NH functional groups were intact after polymerisation [22]. An increase in the concentration of the MAAM (SMP-5) resulted in a sharp increase of the peak of the N-H bending vibration intensity, thus proving the higher density of amide groups inside the polymer network (Figure 3a). This also applied in Figure 4a, when the amount of crosslinking ratio was decreased (SMP-6), leading to higher compactness of amide groups too. X-ray photoelectron spectroscopy (XPS) of the samples with respect to variation in the concentration of template, monomer and concentration confirmed this finding as revealed in Figures 2b, 3b, and 4b respectively.

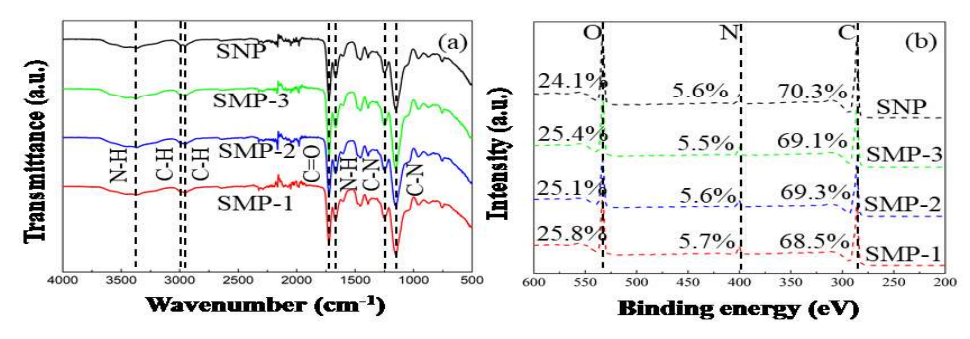


Figure 2: The surface chemical analysis of the samples with respect to template concentration (a) FTR spectra; (b) XPS spectra including the mass percent of Carbon, Oxygen and Nitrogen.

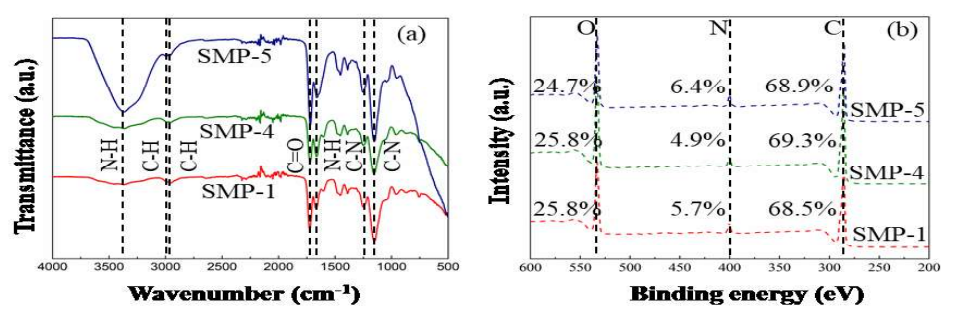


Figure 3: The surface chemical analysis of the samples with respect to monomer concentration (a) FTR spectra; (b) XPS spectra including the mass percent of Carbon, Oxygen and Nitrogen

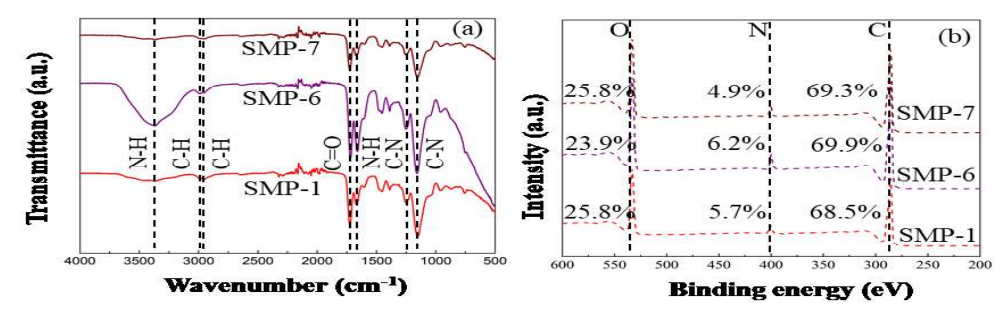


Figure 4: The surface chemical analysis of the samples with respect to crosslinking ratio (a) FTR spectra; (b) XPS spectra including the mass percent of Carbon, Oxygen and Nitrogen

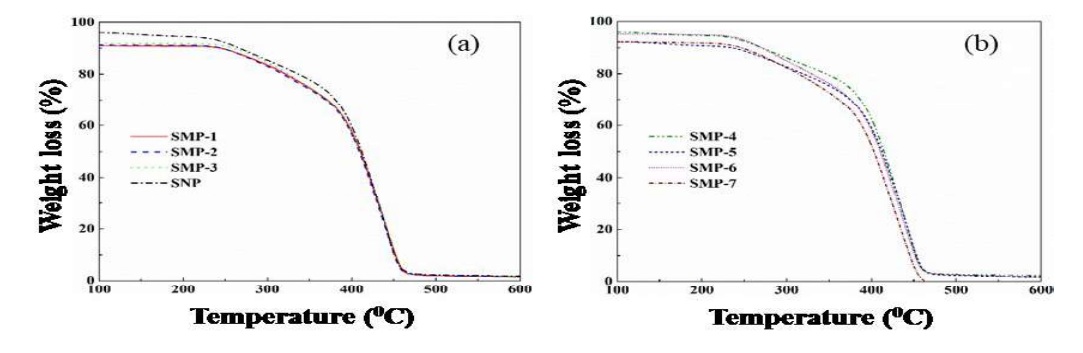


Figure 5: The TGA curves of the samples over the temperature range of 100-600 oC at a heating rate of 10K/min

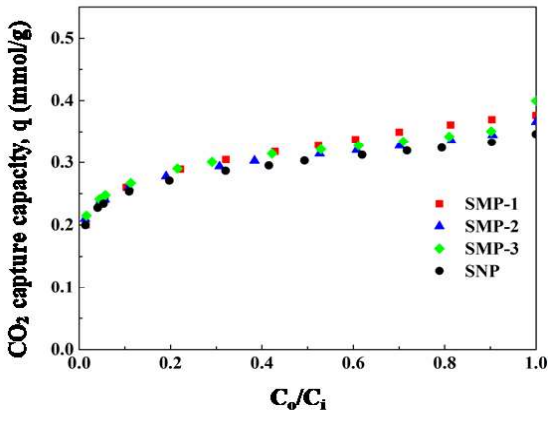


Figure 6: The $\rm CO_2$ adsorption uptake calculated from the breakthrough curves using Eq. (2), showing the variable effect of template concentration. The adsorption temperature was 40 $^{\rm o}$ C and the gas flow rate was 130 mL/min

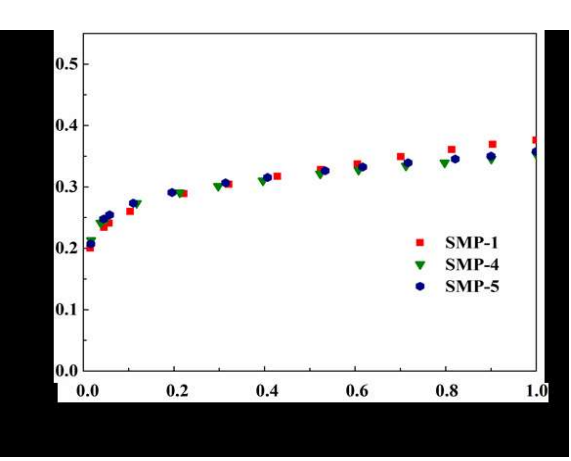


Figure 7: The CO₂ adsorption uptake calculated from the breakthrough curves using Eq. (2), showing the variable effect of monomer concentration. The adsorption temperature was 40 °C and the gas flow rate was 130 mL/min

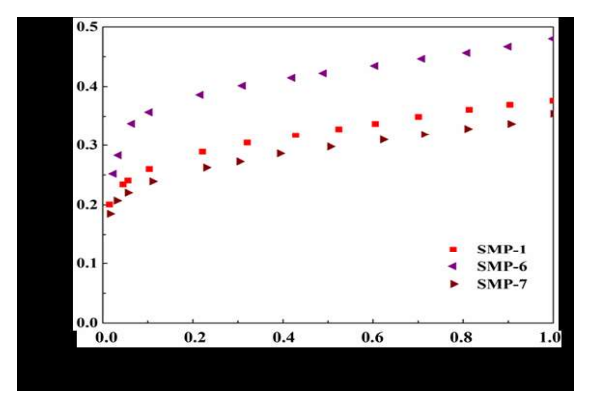


Figure 8: The CO₂ adsorption uptake calculated from the breakthrough curves using Eq. (2), showing the variable effect of the crosslinker concentration. The adsorption temperature was 40 °C and the gas flow rate was 130 mL/min.

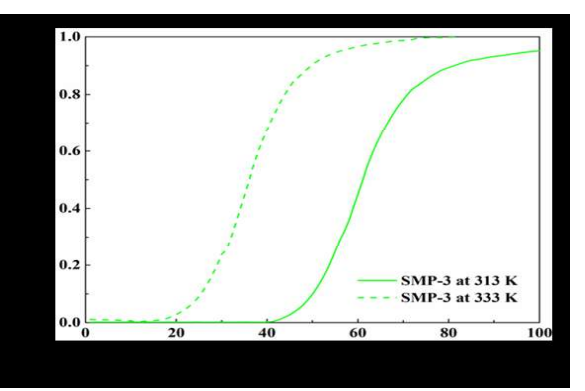


Figure 9: The CO₂ adsorption uptake calculated from the breakthrough curves using Eq. (2), showing the effect of temperature at 313 K and 333 K; the gas flow rate was 130mL/min.

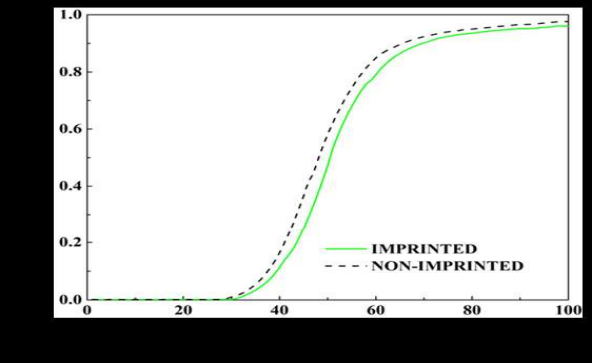


Figure 10: The CO₂ adsorption uptake for imprinted and corresponding non-imprinted polymer calculated from the breakthrough curves using Eq. (2). The adsorption temperature was 40 °C and the gas flow rate was 130mL/min

The thermogravimetric analysis (TGA) curves of the adsorbents shown thermal stability of the SMPs with no significant weight loss up to 513 K (Figure 5). Thus, as compared with previous works earlier reported, the SMPs are thermally stable [8]. Complete degradation

occurred above 450 $^{\circ}$ C for all the samples. Helium pycnometer was used to measure the average density of the adsorbents, and the average value obtained is $\simeq 1.30 \text{ g/cm}^3$.

B. Dynamic CO₂ Adsorption Assessment

The CO₂ adsorption was performed in a stainless steel fixed bed adsorption column and the equilibrium CO₂ capture capacity (Figure S1), *q* (mmol/g) was determined using Equation 1 [15].

$$q = \frac{QC_i t_{ad}}{m_s} \tag{1}$$

where m_s (g) is the mass of the adsorbents in the adsorption column of the fixed bed, t_{ad} is the breakthrough time in an ideal adsorption column, Q (mL/min) is the gas flow rate of the feed, and C_i (mmol/mL) is the molar concentration of the particles in the feed stream given by:

$$C_i = \frac{p_{y_i}}{RT} \tag{2}$$

where R is the universal gas constant (8.314 J/K.mol), T (K) is the operating temperature, y_i the CO₂ molar fraction in the feed stream, and P (kPa) is the total gas pressure in the reactor (~102 kPa).

The breakthrough time in an ideal adsorption column t_{ad} is given by:

$$t_{ad} = \int_0^\infty \left(1 - \frac{c_0}{c_i}\right) dt \tag{3}$$

where C_o (mmol/mL) is the CO₂ molar concentration in the stream effluent.

The plot of the CO_2 adsorption uptake of the samples with reference to variation in template, monomer and crosslinker over the range of C_o/C_i from 0 to 1 is shown in Figures 6, 7 and 8 respectively. In Figure 6, it is glaring that all template polymers (SMP-1 to SMP-3) have higher CO_2 capture capacity as compared to the non-imprinted (SNP).

Surprisingly, SMP-1 with the average amount of template exhibited maximum capacity

compared to SMP-3 with the highest template. This could have been as a result of the difficulty to completely extract the template out, as the concentration increases. Also, in Figure 8, SMP-6 with the lowest crosslinking density displayed the maximum CO₂ adsorption uptake; this could be connected with the effect of the lowest amide – cross-linking density, leading to higher -NH moieties, thus enhancing the capturing capacity.

The temperature dependence of the adsorbents was also performed for SMP-3 at 333 K and likewise, 313 K (Figure 9). The result showed that as temperature increases, the adsorption capacity decreases as expected [15]. Figure 10 shows the breakthrough curves of the imprinted versus non-imprinted polymer, which also revealed the benefits of adding the template.

I. Conclusion

Facile, inexpensive, non-toxic amide-based polymer imprinted adsorbents were synthesized via bulk polymerisation method. It was revealed that the template significantly increased the SBET, though it causes a reduction in both pore size and pore volume. More so, it is glaring that all imprintedpolymers synthesized have higher adsorption uptake of CO₂ capacity as compared to the non-imprinted (SNP). All the adsorption isotherms showed a typical shape of type II featuring a non-uniform distribution of pore size and were thermally stable up to 518 K. The adsorbents demonstrated high CO₂ selectivity over N₂ and exhibited CO₂ uptake of 0.48 mmol/g at 313 K and partial pressure of 0.15 bar, S_{BET} 399 m²/g, thus suitable for post-combustion CCS.

Acknowledgement

The authors acknowledge the financial support granted by CoERCe, under Innovative UK project Grant and Cambridge Engineering Analysis Design (CEAD) Ltd. The authors also appreciate the technologists at the department of Chemical Engineering, Loughborough University for their support during the entire experimental work. We also say thank you to the Loughborough Materials Characterization Centre (LMCC) for helping out in the characterization of the samples.

Supplementary Information

S1. Dynamic CO₂ adsorption isotherms

Dynamic CO₂ adsorptions were performed on the adsorbents synthesized in a stainless steel fixed-bed column of internal and external diameter of 9.25 mm and 15.8 mm respectively (Figure S1). At both side of the fixed bed were placed 0.035 mm stainless steel mesh and quartz wool. In order to achieve a uniform distribution of temperature along the column, an in-built temperature controller was attached. A mass controller (Alicat Scientific Inc., UK) was also attached to control the gas flow rate along the column. Prior to each test, the column was packed with 2 g of the adsorbents, and purged with N₂ at 393 K and 130 mL/min for 90 min; then cooled down to the desired adsorption temperature. CO2 adsorption was carried out by flowing 15 % CO₂ / 85 % N₂ (v/v) simulated gas mixture at 130 mL/min into adsorption column until equilibrium is reached. The CO₂ concentration in the outlet stream was monitored using a CO2 infrared analyser (Quantek Instruments, USA). The desorption was performed by purging the adsorbents with nitrogen at 393 K and 130 mL/min for 90 min. As a confirmation that the CO2 is totally desorbed, a CO2 saturated adsorbent was exposed to N2 at 60 mL/h, 298-361 K. Over the temperature range of 298 -327 K, the adsorbed CO_2 was completely removed and above 327 K, no CO_2 was detected in the effluent stream again.

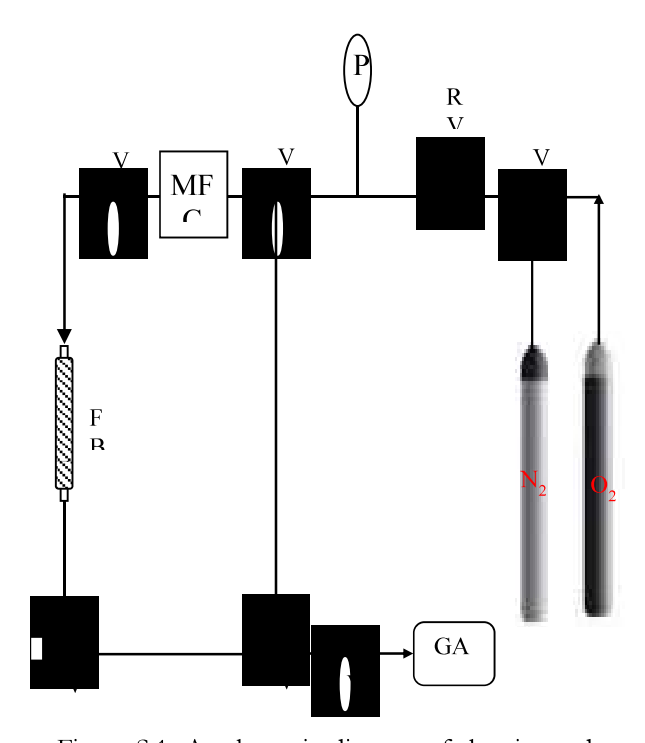


Figure S.1. A schematic diagram of the rig used to test the dynamic CO_2 sorption capacity of the synthetized adsorbents P: pressure gauge; MFC: mass flow controller; FB: fixed bed column couple with heating system; GA: CO_2 gas analyser; V: 3-way valves; and RV: relief valve.

References

- [1] Tseng, R.L., Wu, F.C. and Juang, R.S. "Adsorption of CO₂ at Atmospheric Pressure on Activated Carbons Prepared from Melamine-Modified Phenol–Formaldehyde Resins", *Sep. Purif. Technol.*, vol. 140, 2015, pp. 53–60.
- [2] Sreenivasulu, B., Gayatri, D.V., Sreedhar, I. and Raghavan, K.V. "A Journey into the Process and Engineering Aspects of Carbon Capture Technologies", Renew. Sustain. Energy Rev., vol. 41, 2015, pp. 1324–1350.
- [3] Songolzadeh, M., Soleimani, M., Ravanchi, M.T. and Songolzadeh, R. "Carbon Dioxide Separation from Flue Gases: A Technological

- Review Emphasizing Reduction in Greenhouse Gas Emissions", Sci. World J., vol. 2014, 2014, pp. 1-34.
- [4] Bui, M. *et al.*, "Carbon Capture and Storage (CCS): The Way Forward", *Energy Environ. Sci.*, vol. 11, no. 5, 2018, pp. 1062–1176.
- [5] Chang, F.Y., Chao, K.J., Cheng, H.H. and Tan C.S. "Adsorption of CO₂ onto Amine-Grafted Mesoporous Silicas", Sep. Purif. Technol., vol. 70, no. 1, 2009, pp. 87–95.
- [6] Wang, W., Yuan, Y., Sun, F.X. and Zhu, G.S. "Targeted Synthesis of Novel Porous Aromatic Frameworks with Selective Separation of CO₂ /CH₄ and CO₂ /N₂", Chinese Chem. Lett., vol. 25, no. 11, 2014, pp. 1407–1410.
- [7] Wang, Q., Luo, J., Zhong, Z. and Borgna, A. "CO₂ Capture by Solid Adsorbents and Their Applications: Current Status and New Trends", *Energy Environ. Sci.*, vol. 4, no. 1, 2011, pp. 42–55.
- [8] Zhao, Y., Shen, Y., Bai, L., Hao, R. and Dong, L. "Synthesis and CO₂ Adsorption Properties of Molecularly Imprinted Adsorbents", *Environ. Sci. Technol.*, vol. 46, no. 3, 2012, pp. 1789–1795.
- [9] Nabavi, S.A., Vladisavljević, G.T., Wicaksono, A., Georgiadou, S. and Manović, V. "Production of Molecularly Imprinted Polymer Particles with Amide-Decorated Cavities for CO₂ Capture Using Membrane Emulsification/Suspension Polymerisation", Colloids Surfaces A Physicochem. Eng. Asp., vol. 521, 2017, pp. 231–238.
- [10] Fayemiwo, K.A. et al. "Eco-Friendly Fabrication of a Highly Selective Amide-Based Polymer for CO₂ Capture", Ind. Eng. Chem. Res., vol. 58, no. 39, 2019.
- [11] Fayemiwo, K.A., Chiarasumran, N., Nabavi, S.A., Manović V., Benyahia, В. and Vladisavljević, G.T. "CO₂ Capture Performance and Environmental Impact of Copolymers of Glycol Ethylene Dimethacrylate with Acrylamide, Methacrylamide and Triallylamine", J. Environ. Chem. Eng., 2019, pp. 103536.

- [12] Adánez-Rubio, I., Abad, A., Gayán, P., De Diego, L.F., García-Labiano, F. and Adánez, J. "Biomass Combustion with CO₂ Capture by Chemical Looping with Oxygen Uncoupling (CLOU)", Fuel Process. Technol., vol. 124, 2014, pp. 104–114.
- [13] Antzara, A., Heracleous, E., Bukur, D.B. and Lemonidou, A.A. "Thermodynamic Analysis of Hydrogen Production via Chemical Looping Steam Methane Reforming Coupled with in Situ CO₂ Capture", *Int. J. Greenh. Gas Control*, vol. 32, 2015, pp. 115–128.
- [14] Nabavi, S.A., Vladisavljević, G.T., Zhu, Y. and Manović, V., "Synthesis of Size-Tunable CO₂-Philic Imprinted Polymeric Particles (MIPs) for Low-Pressure CO₂ Capture Using Oil-in-Oil Suspension Polymerization", Environ. Sci. Technol., vol. 51, no. 19, 2017, pp. 11476–11483.
- [15] Nabavi, S.A., Vladisavljević, G.T., Eguagie, E.M., Li, B., Georgiadou, S. and Manović, V. "Production of Spherical Mesoporous Molecularly Imprinted Polymer Particles Containing Tunable Amine Decorated Nanocavities with CO₂ Molecule Recognition Properties", *Chem. Eng. J.*, vol. 306, 2016, pp. 214–225.
- [16] Cormack, P.A.G. and Elorza, A.Z. "Molecularly Imprinted Polymers: Synthesis and Characterisation", J. Chromatogr. B Anal. Technol. Biomed. Life Sci., vol. 804, no. 1, 2004, pp. 173–182.
- [17] Cormack, P.A.G., Elorza, A.Z., Spivak, D.A., MAYES, A. and Whitcombe, M. "Synthetic Strategies for the Generation of Molecularly Imprinted Organic Polymers", Adv. Drug Deliv. Rev., vol. 57, no. 12, 2005, pp. 173–182.
- [18] Yan, H. and Row, K.H., "Characteristic and Synthetic Approach of Molecularly Imprinted Polymer", *Int. J. Mol. Sci.*, vol. 7, no. 5, 2006, pp. 155–178.
- [19] Zhao, Y., Shen, Y., Ma, G. and Hao, R. "Adsorption Separation of Carbon Dioxide from Flue Gas by a Molecularly Imprinted Adsorbent", *Environ. Sci. Technol.*, vol. 48, no. 3, 2014, pp. 1601–1608.

- [20] Zhang, Y. and Lei, J. "Synthesis and Evaluation of Molecularly Imprinted Polymeric Microspheres for Chloramphenicol by Aqueous Suspension Polymerization as a High Performance Liquid Chromatography Stationary Phase", Bull. Korean Chem. Soc., vol. 34, no. 6, 2013, pp. 1839–1844.
- [21] Scorrano, S., Mergola, L., Del Sole, R. and Vasapollo, G. "Synthesis of Molecularly Imprinted Polymers for Amino Acid Derivates by Using Different Functional Monomers", *Int. J. Mol. Sci.*, vol. 12, no. 12, 2011, pp. 1735–1743.
- [22] Fayemiwo, K.A. et al., "Nitrogen-Rich Hyper-Crosslinked Polymers for Low-Pressure CO₂ Capture", Chem. Eng. J., vol. 334, 2018, pp. 2004–2013.
- [23] Qi, G., Fu, L. and Giannelis, E.P. "Sponges with Covalently Tethered Amines for High Efficiency Carbon Capture", Nat. Commun., vol. 5, 2014, pp. 5796.
- [24] Ben, T. et al., "Targeted Synthesis of a Porous Aromatic Framework with High Stability and Exceptionally High Surface Area", Angew. Chemie Int. Ed., vol. 48, no. 50, 2009, pp. 9457–9460.
- [25] Chen, X., Qiao, S., Du, Z., Zhou, Y. and Yang, R. "Synthesis and Characterization of Functional Thienyl-Phosphine Microporous Polymers for Carbon Dioxide Capture", Macromol. Rapid Commun., vol. 34, no. 21, 2013, pp. 1181–1185.
- [26] Weidenthaler, C. "Pitfalls in the Characterization of Nanoporous and Nanosized Materials," *Nanoscale*, vol. 3, no. 3, 2011, pp. 792–810.